16th European Signal Processing Conference (EUSIPCO 2008), Lausanne, Switzerland, August 25-29, 2008, copyright by EURASIP

JOINT FREQUENCY AND 2-D ANGLE ESTIMATION BASED ON VECTOR SENSOR ARRAY WITH SUB-NYQUIST TEMPORAL SAMPLING

Fei Ji[1], *Carrson C. Fung*[2], *Sam Kwong*[3] *and Chi-Wah Kok*[4]

[1]School of Electronic and Information Engineering, South China University of Technology, Guangdong, China, email: *eefeiji@scut.edu.cn*

[2] Dept. of Electronics Engineering, National Chiao Tung University, Hsinchu, Taiwan, 300, email: *c.fung@ieee.org*

[3] Dept. of Computer Science, City University of Hong Kong, Hong Kong, email: *cssamk@cityu.edu.hk*

[4] Dept. of Electronic Engineering, City University of Hong Kong, Hong Kong, email: *eekok@ieee.org*

ABSTRACT

A novel ESPRIT based algorithm is proposed to jointly estimate 2-dimensional direction-of-arrivals (2-D DOAs) and frequencies of the incoming superimposed complex sinusoidal signals using a sparse uniform linear array of electromagnetic vector-sensors. The proposed method is based on a matrix pencil pair of temporally displaced data sets that are collected from the electromagnetic vector sensor array, where the DOA and frequency estimates can be estimated unambiguously from the eigenvectors and eigenvalues of the matrix pencil even when the interelement spacing is more than half wavelength. A second algorithm is proposed to resolve the ambiguity problem in the frequency estimates when the temporal sampling rate is less than half of the Nyquist rate of the signal, i.e. the sampling rate is less than the maximum frequency of the signal. Simulation results support the proposed algorithms and show that the 2-D DOA and frequency estimates are asymptotically unbiased and have a low variance.

1. INTRODUCTION

Joint two-dimensional (elevation and azimuth angle) direction-of-arrival (2-D DOA) and frequency estimation of multiple superimposed complex sinusoidal signals has applications in many areas such as wireless communications [1], radio astronomy, ultrasound imaging, sonar and radar. Much work has been reported on joint estimation of 2-D DOA and frequency parameters using scalar-sensor array [2, 3] and vector-sensor array [4, 5, 6, 7]. In narrowband systems, a sub-Nyquist temporal or spatial sampling rate can improve the accuracy of the frequency or angle estimates, but lead to frequency or spatial aliasing, thus, causing ambiguity in the frequency or spatial estimates [2, 3]. It is thus advantageous to be able to estimate these parameters using an array of sensors that are aliased either spatially, temporally or both. A multiresolution ESPRIT algorithm was proposed in [3] where two different sensor spacings were used, i.e. $\Delta x \leq \frac{\lambda}{2}$ and $\Delta x > \frac{\lambda}{2}$, where Δx denotes the inter-sensor spacing, and λ is the wavelength of the signal. Its results have shown that using two different spatial resolutions can improve accuracy of the estimates. [5] and [6] have shown that using multiple or a single electromagnetic vector sensors can improve estimation performance over scalar-sensors because 1) one vector-sensor measurements results in a 6×1 steering vector which is equivalent to having a six-element array of sensor, 2) the array manifolds of vector-sensor are independent of the impinging signals' frequency spectra, and 3) signals having identical DOAs but different polarization can be distinguished by exploiting the polarization diversity property of an uni-vector-sensor.

In this paper, a novel ESPRIT based algorithm is proposed to jointly estimate 2-D DOA and frequency of the incoming multiple superimposed complex sinusoidal signal using a sparse uniform array of electromagnetic vector-sensors. The 2-D DOA and frequency estimates are estimated unambiguously from the eigenvectors and eigenvalues of the matrix pencil given arbitrary interelement spacing and when the temporal sampling is at half the Nyquist rate. This has applications in distributed sensor array where the sensors can be located sparsely over a wide region of space.

Since the frequencies of the impinging signal have to be estimated, it is possible the signal will be insufficiently sampled temporally at the sensor array, which causes ambiguity in the frequency estimates. Therefore, another algorithm is proposed to allow unambiguous estimation of 2-D DOA and frequency when the received signal is temporally undersampled. We will show this is possible if the interelement spacing is confined to be equal to or less than half the signal's wavelength (the shortest one). Since the frequency of the impinging signal is unknown, this method will guarantee the frequency can be estimated unambiguously as long as the receiver has knowledge about the upper bound of the incoming signal's frequency, the interelement constraint is satisfied and the SNR is high enough. The proposed frequency disambiguation algorithm makes use of the unambiguous DOA information embedded in the impinging electromagnetic field components. Simulation results of the proposed algorithms show that the 2-D DOA and frequency estimates are asymptotically unbiased and have low variance.

The proposed algorithms are described in the next section, followed by the simulation results in Section 3. The paper will be concluded in Section 4.

2. METHODOLOGY

Since the notations used in this paper are identical to the ones in [6], therefore, for the sake of space, the reader should refer to [6] for a complete clarification on all of the notations. The impinging K signals are assumed to be uncorrelated, narrowband and are completely polarized transverse electromagnetic plane waves with different baseband modulated frequencies. The signals travel through a homogeneous isotropic medium, incident on a linear array of equally spaced and identical electromagnetic vector-sensors. The k^{th} signal is characterized by its six component electromagnetic field vector

$$\mathbf{g}_k \triangleq \begin{bmatrix} \sin\gamma_k \cos\theta_k \cos\phi_k e^{j\eta_k} - \cos\gamma_k \sin\phi_k \\ \sin\gamma_k \cos\theta_k \sin\phi_k e^{j\eta_k} + \cos\gamma_k \cos\phi_k \\ -\sin\gamma_k \sin\theta_k e^{j\eta_k} \\ -\cos\gamma_k \cos\theta_k \cos\phi_k - \sin\gamma_k \sin\phi_k e^{j\eta_k} \\ -\cos\gamma_k \cos\theta_k \sin\phi_k + \sin\gamma_k \cos\phi_k e^{j\eta_k} \\ \cos\gamma_k \sin\theta_k \end{bmatrix},$$

where $0 \leq \theta_k < \pi$ is the signal's elevation angle measured from the vertical z-axis, $0 \leq \phi_k < 2\pi$ is the azimuth angle, $0 \leq \gamma_k < \pi/2$ is the auxiliary polarization angle, and $-\pi \leq \eta_k < \pi$ is the polarization phase difference. Note that $\mathbf{g}_k$ is independent of the signal frequency. Defining $\mathbf{e}_k \triangleq \begin{bmatrix} e_{xk} & e_{yk} & e_{zk} \end{bmatrix}^T$ and $\mathbf{h}_k \triangleq \begin{bmatrix} h_{xk} & h_{yk} & h_{zk} \end{bmatrix}^T$ as the electric and magnetic field vector for the k^{th} signal, respectively,

The work described in this paper has been supported by the National Natural Science Foundation of China Grant 60672065, National Science Council Grant 96-2221-E-009-053; City University Strategic Grant 7001955 and Competitive Earmark Research Grant PolyU 5133/02E.

the k^{th} source's direction of propagation can be expressed using the Poynting vector

$$\mathbf{p}_k = \frac{\mathbf{e}_k}{\|\mathbf{e}_k\|} \times \frac{\mathbf{h}_k^*}{\|\mathbf{h}_k\|} = \begin{bmatrix} u_k \\ v_k \\ w_k \end{bmatrix} = \begin{bmatrix} \sin\theta_k \cos\phi_k \\ \sin\theta_k \sin\phi_k \\ \cos\theta_k \end{bmatrix},$$

where * denotes complex conjugation and u_k, v_k, w_k denotes the direction cosine along the $x-$, $y-$ and $z-$axis, respectively. To account for the phase difference between the impinging signal arriving at different sensors, we define a spatial phase factor

$$\begin{aligned} q_m(\theta_k, \phi_k) &= e^{j2\pi f_k (m-1)\Delta x u_k / c} \\ &= e^{j2\pi f_k (m-1)\Delta x \sin\theta \cos\phi_k / c} \end{aligned}$$

for the k^{th} signal at the m^{th} vector sensor located at $(m-1)\Delta x$, where f_k is the frequency of the k^{th} signal, c is the speed of light and $m = 1, 2, \ldots, M$. Therefore, the m^{th} vector sensor output, $\mathbf{z}_m(t) \in \mathbb{C}^{6\times 1}$, which is composed of a sum of K narrowband far-field signals corrupted by additive white noise, $\mathbf{n}_m(t) \in \mathbb{C}^{6\times 1}$, can be written as

$$\mathbf{z}_m(t) = \sum_{k=1}^{K} \mathbf{g}_k s_k(t, f_k) q_m(\theta_k, \phi_k) + \mathbf{n}_m(t), \tag{1}$$

where $s_k(t, f_k) = \sqrt{P_k} e^{j(2\pi f_k t + \varphi_k)}$ is the impinging signal, P_k is the k^{th} source's energy, and φ_k is the random phase of the k^{th} signal, which is uniformly distributed. A time-delayed version of $\mathbf{z}_m(t)$ can be defined similarly as

$$\begin{aligned} \mathbf{z}_m(t+\Delta T) &= \sum_{k=1}^{K} \mathbf{g}_k s_k(t+\Delta T, f_k) q_m(\theta_k, \phi_k) + \mathbf{n}_m(t+\Delta T) \\ &= \sum_{k=1}^{K} \mathbf{g}_k s_k(t, f_k) q_m(\theta_k, \phi_k) e^{j2\pi f_k \Delta T} + \mathbf{n}_m(t+\Delta T). \end{aligned} \tag{2}$$

Using (1) and (2), a $12M \times N$ temporal-spatial matrix

$$\mathbf{Z} = \begin{bmatrix} \mathbf{X} \\ -- \\ \mathbf{Y} \end{bmatrix} = \begin{bmatrix} \mathbf{x}(t_1) \ \ldots \ \mathbf{x}(t_N) \\ - - - - - - - \\ \mathbf{y}(t_1) \ \ldots \ \mathbf{y}(t_N) \end{bmatrix} \tag{3}$$

can be formed, where

$$\begin{aligned} \mathbf{x}(t) &= \left[\mathbf{z}_1^T(t)\, \mathbf{z}_2^T(t) \cdots \mathbf{z}_M^T(t)\right]^T = \mathbf{A}\mathbf{s} + \mathbf{n}_1 \\ \mathbf{y}(t) &= \left[\mathbf{z}_1^T(t+\Delta T)\, \mathbf{z}_2^T(t+\Delta T) \cdots \mathbf{z}_M^T(t+\Delta T)\right]^T \\ &= \mathbf{A}\mathbf{\Phi}\mathbf{s} + \mathbf{n}_2, \\ \mathbf{A} &= [\mathbf{a}_1\, \mathbf{a}_2 \cdots \mathbf{a}_K] \\ &= [\mathbf{q}(\theta_1, \phi_1) \otimes \mathbf{g}_1 \cdots \mathbf{q}(\theta_K, \phi_K) \otimes \mathbf{g}_K], \\ \mathbf{q}_m(\theta_k, \phi_k) &= \left[1\ e^{j2\pi f_k \Delta x u_k / c} \ \ldots \ e^{j2\pi f_k (M-1)\Delta x u_k / c}\right]^T, \\ \mathbf{s} &= [s_1(t, f_1)\, s_2(t, f_2) \cdots s_K(t, f_K)]^T, \\ \mathbf{\Phi} &= diag\left(e^{j2\pi f_1 \Delta T}, \ldots, e^{j2\pi f_K \Delta T}\right), \\ \mathbf{n}_1 &= \left[\mathbf{n}_1^T(t)\, \mathbf{n}_2^T(t) \ \ldots \ \mathbf{n}_M^T(t)\right]^T, \\ \mathbf{n}_2 &= \left[\mathbf{n}_1^T(t+\Delta T)\, \mathbf{n}_2^T(t+\Delta T) \cdots \mathbf{n}_M^T(t+\Delta T)\right]^T, \end{aligned}$$

and $\otimes$ denotes the Kronecker product. From (3), it is clear that the columns of $\mathbf{X}$ and $\mathbf{Y}$ are combination of the columns of $\mathbf{A}$ and $\mathbf{A\Phi}$, respectively. Thus, the signal subspace of $\mathbf{X}$ is spanned by the columns of $\mathbf{A}$, and similarly, the signal subspace of $\mathbf{Y}$ is spanned by the columns of $\mathbf{A\Phi}$. Define $\mathbf{E}_1$ and $\mathbf{E}_2$ as the signal subspace matrix for $\mathbf{X}$ and $\mathbf{Y}$, respectively. Assuming $K < 6M < N$, where N is the number of snapshots taken, $\mathbf{E}_1$ and $\mathbf{E}_2$ can be obtained by performing the singular value decomposition (SVD) on $\mathbf{X}$ and $\mathbf{Y}$ such that $\mathbf{E}_1 =$ first K columns of $\mathbf{U}_\mathbf{X}$ and $\mathbf{E}_2 =$ first K columns of $\mathbf{U}_\mathbf{Y}$, where $\mathbf{X} = \mathbf{U}_\mathbf{X}\mathbf{\Sigma}_\mathbf{X}\mathbf{V}_\mathbf{X}^H$ and $\mathbf{Y} = \mathbf{U}_\mathbf{Y}\mathbf{\Sigma}_\mathbf{Y}\mathbf{V}_\mathbf{Y}^H$. Since the columns of $\mathbf{E}_1$ and $\mathbf{A}$ span the same K-dimensional subspace, and the columns of $\mathbf{E}_2$ and $\mathbf{A\Phi}$ span the same K-dimensional subspace, they are related by an arbitrary non-singular $K \times K$ matrix, $\mathbf{T}$, such that

$$\begin{bmatrix} \mathbf{E}_1 \\ \mathbf{E}_2 \end{bmatrix} = \begin{bmatrix} \mathbf{A} \\ \mathbf{A\Phi} \end{bmatrix} \mathbf{T}. \tag{4}$$

To obtain the frequency estimates $f_1, f_2, \ldots, f_K$, we need to solve for $\mathbf{\Phi}$. Note that $\mathbf{E}_1$ and $\mathbf{E}_2$ have full column rank and they span their respective K-dimensional subspaces of $\mathbf{X}$ and $\mathbf{Y}$. Since $\mathbf{X}$ and $\mathbf{Y}$ are related by a subspace rotation matrix $\mathbf{\Phi}$, therefore, $\mathbf{E}_1$ and $\mathbf{E}_2$ must also be related by a similar, but different, full rank $K \times K$ rotation matrix $\mathbf{\Psi}$, i.e.

$$\mathbf{E}_1 \mathbf{\Psi} = \mathbf{E}_2. \tag{5}$$

Substitute (4) into (5), we have

$$\underbrace{\mathbf{AT}}_{\mathbf{E}_1} \mathbf{\Psi} = \underbrace{\mathbf{A\Phi T}}_{\mathbf{E}_2}.$$

Multiply both sides by $(\mathbf{AT})^H$ and solving for $\mathbf{\Phi}$, we get

$$\begin{aligned} \mathbf{T}^H\mathbf{A}^H\mathbf{AT}\mathbf{\Psi} &= \mathbf{T}^H\mathbf{A}^H\mathbf{A\Phi T} \\ \Longrightarrow \mathbf{\Psi} &= (\mathbf{T}^H\mathbf{A}^H\mathbf{AT})^{-1}\mathbf{T}^H\mathbf{A}^H\mathbf{A\Phi T} \\ &= \mathbf{T}^{-1}\mathbf{\Phi T} \\ \Longrightarrow \mathbf{\Phi} &= \mathbf{T\Psi T}^{-1}. \end{aligned} \tag{6}$$

Thus, $\mathbf{\Phi}$ is the eigenvalue matrix of $\mathbf{\Psi}$ with $\mathbf{T}$ as its eigenvector matrix. Using $\mathbf{\Phi}$ and $\mathbf{T}$, the estimates of θ_k and ϕ_k can be obtained by computing $\mathbf{A}$. This can be done by noting from (4) that

$$\begin{aligned} \widehat{\mathbf{A}} &= \mathbf{E}_1\mathbf{T}^{-1} = \mathbf{E}_2\mathbf{T}^{-1}\mathbf{\Phi}^{-1} \\ &= 0.5\left(\mathbf{E}_1\mathbf{T}^{-1} + \mathbf{E}_2\mathbf{T}^{-1}\mathbf{\Phi}^{-1}\right). \end{aligned} \tag{7}$$

The factor $\mathbf{\Phi}^{-1}$ in (7) is to ensure coherent addition of the two sets of signal subspace eigenvectors, $\mathbf{E}_1$ and $\mathbf{E}_2$, and it is crucial to determining the best estimate for $\mathbf{A}$ [6].

2.1 Unambiguous frequency estimation for arbitrary Δx

From (7), the array manifold estimate is written as

$$\begin{aligned} \widehat{\mathbf{a}}_k &= \widehat{\mathbf{q}}(\theta_k, \phi_k) \otimes \widehat{\mathbf{g}}_k = \widehat{\mathbf{q}}(\theta_k, \phi_k) \otimes \begin{bmatrix} \widehat{\mathbf{e}}_k \\ \widehat{\mathbf{h}}_k \end{bmatrix} \\ &= \begin{bmatrix} \widehat{q}_1(\theta_k, \phi_k)\widehat{\mathbf{e}}_k \\ \widehat{q}_1(\theta_k, \phi_k)\widehat{\mathbf{h}}_k \\ \vdots \\ \widehat{q}_M(\theta_k, \phi_k)\widehat{\mathbf{e}}_k \\ \widehat{q}_M(\theta_k, \phi_k)\widehat{\mathbf{h}}_k \end{bmatrix}. \end{aligned}$$

Defining

$$\mathbf{b}_i(k) \triangleq \widehat{q}_i(\theta_k, \phi_k)\widehat{\mathbf{e}}_k \quad \text{and} \tag{8}$$

$$\mathbf{c}_i(k) \triangleq \widehat{q}_i(\theta_k, \phi_k)\widehat{\mathbf{h}}_k \tag{9}$$

and noting that

$$\frac{\mathbf{b}_i(k)}{\|\mathbf{b}_i(k)\|}\times\frac{\mathbf{c}_i^*(k)}{\|\mathbf{c}_i(k)\|} = \frac{\widehat{q}_i(\theta_k,\phi_k)\widehat{\mathbf{e}}_k}{\|\widehat{q}_i(\theta_k,\phi_k)\widehat{\mathbf{e}}_k\|}\times\frac{\widehat{q}_i^*(\theta_k,\phi_k)\widehat{\mathbf{h}}_k}{\|\widehat{q}_i(\theta_k,\phi_k)\widehat{\mathbf{h}}_k\|} = \frac{\widehat{\mathbf{e}}_k}{\|\widehat{\mathbf{e}}_k\|}\times\frac{\widehat{\mathbf{h}}_k^*}{\|\widehat{\mathbf{h}}_k\|},$$

then the estimates for the three direction-cosines are written as $\widehat{\mathbf{p}}_k=[\widehat{u}_k\ \widehat{v}_k\ \widehat{w}_k]^T=\frac{1}{M}\sum_{i=1}^{M}\frac{\mathbf{b}_i(k)}{\|\mathbf{b}_i(k)\|}\times\frac{\mathbf{c}_i^*(k)}{\|\mathbf{c}_i(k)\|}$. The azimuth and elevation angle estimates are all automatically matched without any additional processing. Note that 2-D azimuth-elevation direction finding has been performed without any a priori knowledge about the signal frequencies and the array element spacing Δx is not needed.

From (6), the estimate of the frequency, f_k, can be estimated unambiguously given arbitrary interelement spacing, that is, Δx can be larger than $\lambda_{min}/2$, where λ_{min} corresponds to the smallest wavelength. Denote ψ_k, for $k=1,2,\ldots,K$, as the eigvenvalue of $\mathbf{\Psi}$ such that $\psi_k=e^{j2\pi\widehat{f}_k\Delta T}$. ΔT is then chosen as

$$2\pi f_{max}\Delta T\le 2\pi \Longrightarrow \Delta T\le\frac{1}{f_{max}},$$

where f_{max} is the maximum signal frequency. Then the unambiguous frequency estimates can be obtained as

$$\widehat{f}_{k0}=\begin{cases}\frac{\mathrm{Arg}\{\psi_k\}}{2\pi\Delta T}, & \text{for } \mathrm{Arg}\{\psi_k\}>0\\ \frac{2\pi+\mathrm{Arg}\{\psi_k\}}{2\pi\Delta T}, & \text{for } \mathrm{Arg}\{\psi_k\}\le 0\end{cases}, \qquad (10)$$

where $\mathrm{Arg}\{z\}$ is the principle argument of the complex number z between $-\pi$ and π. ΔT can be expressed as $\Delta T\triangleq N_T/F_s$, where N_T is a positive integer and F_s is the sampling frequency at the sensor array. Given the maximum signal frequency f_{max}, then the Nyquist temporal sampling rate $F_{Nyq}=2f_{max}$. If $N_T=1$, then $\Delta T=1/f_{max}$, such that $F_s=f_{max}$, which is the minimum sampling frequency we can choose.

2.2 Unambiguous frequency estimation using sub-Nyquist sampling

Since the frequencies of the impinging signal have to be estimated, it is possible the signal will be undersampled temporally at the sensor array, which causes ambiguity in the frequency estimates. Below, we proposed another algorithm for our joint 2-D DOA and frequency estimation problem such that the temporal sampling frequency F_s can be further reduced without introducing ambiguity in the frequency estimates, i.e. $F_s<f_{max}$. We shall show that this can be done only when the interelement spacing is equal to or less than $\lambda_{min}/2$. This can be shown by setting $F_s<F_{Nyq}/2$ and $N_T\ge 1$, so that $2\pi f_{max}\Delta T>2\pi$, which leads to cyclic ambiguity in the frequency estimates, i.e.

$$\widehat{f}_k(n_f)=\widehat{f}_{k0}+\frac{n_f}{\Delta T},\quad 1\le n_f\le\left\lfloor\left(f_{max}-\widehat{f}_{k0}\right)\Delta T\right\rfloor, \qquad (11)$$

where $\lfloor x\rfloor$ is the largest integer not greater than x. Decomposing (8) and (9) into three components,

$$\mathbf{b}_i(k)=\begin{bmatrix}b_{ix}(k)\\ b_{iy}(k)\\ b_{iz}(k)\end{bmatrix}=\widehat{q}_i(\theta_k,\phi_k)\begin{bmatrix}\widehat{e}_{xk}\\ \widehat{e}_{yk}\\ \widehat{e}_{zk}\end{bmatrix}\quad\text{and}$$

$$\mathbf{c}_i(k)=\begin{bmatrix}c_{ix}(k)\\ c_{iy}(k)\\ c_{iz}(k)\end{bmatrix}=\widehat{q}_i(\theta_k,\phi_k)\begin{bmatrix}\widehat{h}_{xk}\\ \widehat{h}_{yk}\\ \widehat{h}_{zk}\end{bmatrix},$$

the estimates for the spatial phase factor become

$$\widehat{q}(\theta_k,\phi_k) = \frac{1}{5(M-1)}\sum_{i=1}^{M-1}\left(\frac{b_{(i+1)x}}{b_{ix}}+\frac{b_{(i+1)y}}{b_{iy}}+\frac{c_{(i+1)x}}{c_{ix}}+\frac{c_{(i+1)y}}{c_{iy}}+\frac{c_{(i+1)z}}{c_{iz}}\right).$$

The term $\frac{b_{(i+1)z}}{b_{iz}}$ does not have to be included in the above equation because when $\gamma_k=0$, e_{zk} will be equal to 0. n_f can be estimated by noting that since $\Delta x\le\lambda_{min}/2$, then $-\pi\le Arg(\widehat{q}(\theta_k,\phi_k))<\pi$, so that

$$\widehat{n}_f=\arg\min_{n_f}\left|e^{j2\pi\left(\widehat{f}_{k0}+\frac{n_f}{\Delta T}\right)\Delta x\widehat{u}_k/c}-\widehat{q}(\theta_k,\phi_k)\right|. \qquad (12)$$

As a result, the disambiguated frequency estimates can be obtained as

$$\widehat{f}_k=\widehat{f}_{k0}+\widehat{n}_f/\Delta T.$$

It can be seen from (12) that the estimation accuracy of $\widehat{n}_f$ depends on the estimation accuracy of $\widehat{f}_{k0}$, $\widehat{u}_k$ and $\widehat{q}(\theta_k,\phi_k)$. According to [8], the accuracy of $\widehat{\mathbf{A}}$ in (7) is adversely affected when the SNR is low. Since estimates $\widehat{u}_k$ and $\widehat{q}(\theta_k,\phi_k)$ are deduced from $\widehat{\mathbf{A}}$, thus, in low SNR condition, the estimate for f_k can be adversely affected. The same situation applies to $\widehat{n}_f$ as well so that the disambiguation algorithm for the frequency estimate is influenced by the SNR and under low SNR, it can fail if the number of snapshots N does not lead to consistent sample averages in the estimation of the signal subspaces $\mathbf{E}_1$ and $\mathbf{E}_1$.

3. RESULTS

The performance of the proposed algorithms is illustrated by the following three simulations which show the standard deviation and bias of the 2-D DOA and frequency estimates. The K signal sources are monochromatic uncorrelated sources with energy P_k normalized to 1, for $k=1,2,\ldots,K$. The integer N_T is set to 1. The total least-squares ESPRIT algorithm [8] is used in all the simulations. A total of 400 snapshots and 400 trials were utilized for all the simulations.

In the first simulation, we show the case for unambiguous frequency estimates by setting the temporal sampling frequency to half the Nyquist rate. K and M are set to 3 and 4, respectively. The parameters for the three signals are: $\{\theta_1,\theta_2,\theta_3\}=\{100^\circ,30^\circ,76.7^\circ\}$, $\{\phi_1,\phi_2,\phi_3\}=\{60^\circ,335^\circ,69.1^\circ\}$, $\{\gamma_1,\gamma_2,\gamma_3\}=\{0^\circ,45^\circ,45^\circ\}$, $\{\eta_1,\eta_2,\eta_3\}=\{0^\circ,0^\circ,90^\circ\}$, and $\{f_1,f_2,f_3\}=\{6.9,7.1,7.3\}$. Figure 1 shows the results for standard deviation of the the direction cosine estimates, frequency estimates and the bias for the direction cosine estimate and frequency estimates for the 3 sources. The temporal sampling frequency is set to $F_s=F_{Nyp}/2=f_{max}=7.3$. The sensor spacing $\Delta x=\frac{7.3c}{2f_{max}}$. As the figures show, the accuracy of the estimates improves as the SNR increases. In addition, all the estimates are asymptotically unbiased.

In the second simulation, we again show the case for unambiguous frequency estimates by setting the temporal sampling frequency to half the Nyquist rate, i.e. $F_s=F_{Nyq}/2=f_{max}=0.32$. This time, $K=8$ and $M=2$. The sensor spacing is $\Delta x=\frac{3.2c}{2f_{max}}$. The parameters for the eight signals are: $\{\theta_1,\theta_2,\theta_3,\theta_4,\theta_5,\theta_6,\theta_7,\theta_8\}=\{20^\circ,58.6^\circ,26.7^\circ,51.4^\circ,30^\circ,48.6^\circ,35^\circ,100^\circ\}$,
$\{\phi_1,\phi_2,\phi_3,\phi_4,\phi_5,\phi_6,\phi_7,\phi_8\}=\{40^\circ,57.4^\circ,69.1^\circ,75.3^\circ,106.3^\circ,170.8^\circ,18^\circ,70^\circ\}$,
$\{\gamma_1,\gamma_2,\gamma_3,\gamma_4,\gamma_5,\gamma_6,\gamma_7,\gamma_8\}=\{70^\circ,0^\circ,90^\circ,145^\circ,45^\circ,45^\circ,45^\circ,80^\circ\}$,
$\{\eta_1,\eta_2,\eta_3,\eta_4,\eta_5,\eta_6,\eta_7,\eta_8\}=\{55^\circ,0^\circ,0^\circ,0^\circ,90^\circ,90^\circ,45^\circ,60^\circ\}$,
and $\{f_1,f_2,f_3,f_4,f_5,f_6,f_7,f_8\}=\{0.25,0.26,0.27,0.28,0.29,0.30,0.31,0.32\}$. Figure 2 shows the results for standard deviation of the direction cosine estimates, frequency estimates and the bias for the direction cosine estimates and frequency estimates for the 8 sources. Once again, the accuracy of the estimates improves as the SNR increases. However, the bias of the estimates does not seem to be affected by the SNR, as in the case for the first simulation. This is due to the fact that for $M\ge 2$ vector-sensor arrays, there exist $(3M+1)$ steering vectors with distinct DOA's that are linearly dependent [9]. This causes the estimates for the direction-cosine and frequency to be biased.

Note that the number of source signal, K, that the proposed algorithm can detect can be greater than the number of sensors, M. This is different from the result in [6] where the maximum number

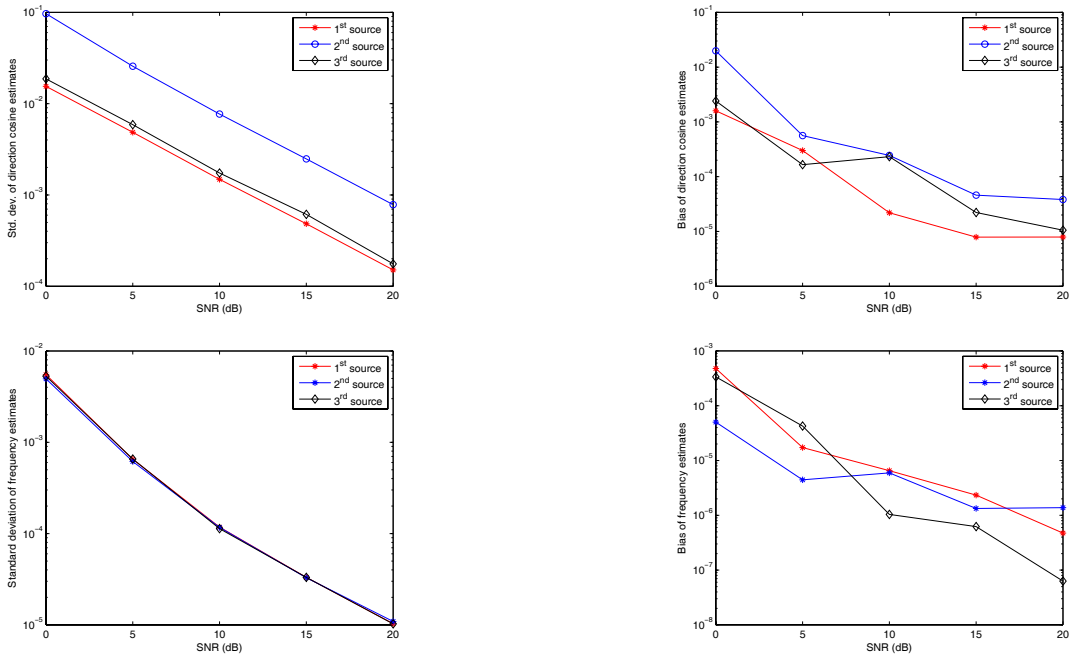

Figure 1: Standard deviation and bias of direction cosine and frequency estimates for $K = 3$, $M = 4$ with temporal sampling rate of $F_{Nyq}/2$ (from left to right, top to bottom): standard deviation of direction estimates, bias of direction cosine estimates, standard deviation of frequency estimates, bias of frequency estimates.

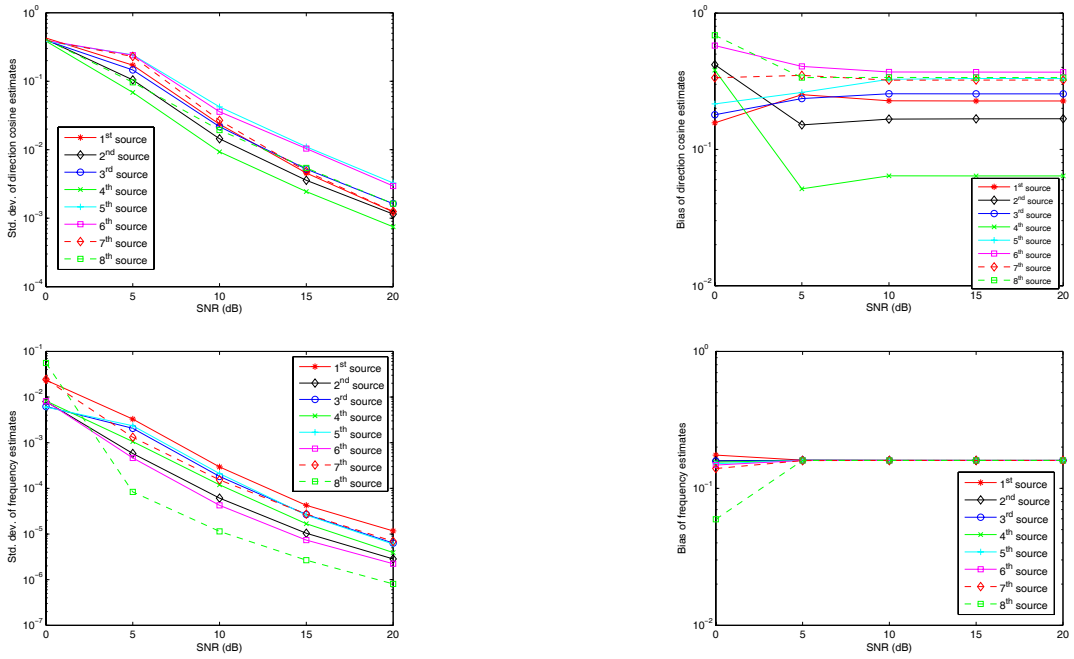

Figure 2: Standard deviation and bias of direction cosine and frequency estimates for $K = 8$, $M = 2$ with temporal sampling rate of $F_{Nyq}/2$ (from left to right, top to bottom): standard deviation of direction estimates, bias of direction cosine estimates, standard deviation of frequency estimates, bias of frequency estimates.

of signals that can be detected is less than M because vector-sensor array offers more degree of freedom $(6M-K)$ than the $6-K$ degree of freedom one can obtain from the uni-vector-sensor.

In the third simulation, the sub-Nyquist disambiguation algorithm was used for three signals impinging on four vector sensors, i.e. $K = 3$ and $M = 4$. The parameters for the three signals are: $\{\theta_1, \theta_2, \theta_3\} = \{30^\circ, 140^\circ, 100^\circ\}$, $\{\phi_1, \phi_2, \phi_3\} = \{40^\circ, 50^\circ, 120^\circ\}$, $\{\gamma_1, \gamma_2, \gamma_3\} = \{0^\circ, 45^\circ, 45^\circ\}$, $\{\eta_1, \eta_2, \eta_3\} = \{0^\circ, 90^\circ, 0^\circ\}$, and $\{f_1, f_2, f_3\} = \{3, 7.5, 8\}$. The temporal sampling frequency is set to $F_s = F_{Nyp}/4 = 4$. The sensor spacing is $\Delta x = \frac{c}{2f_{max}}$. Figure 3 shows the results for standard deviation of the direction cosine estimates, frequency estimates and the bias for the direction cosine estimate

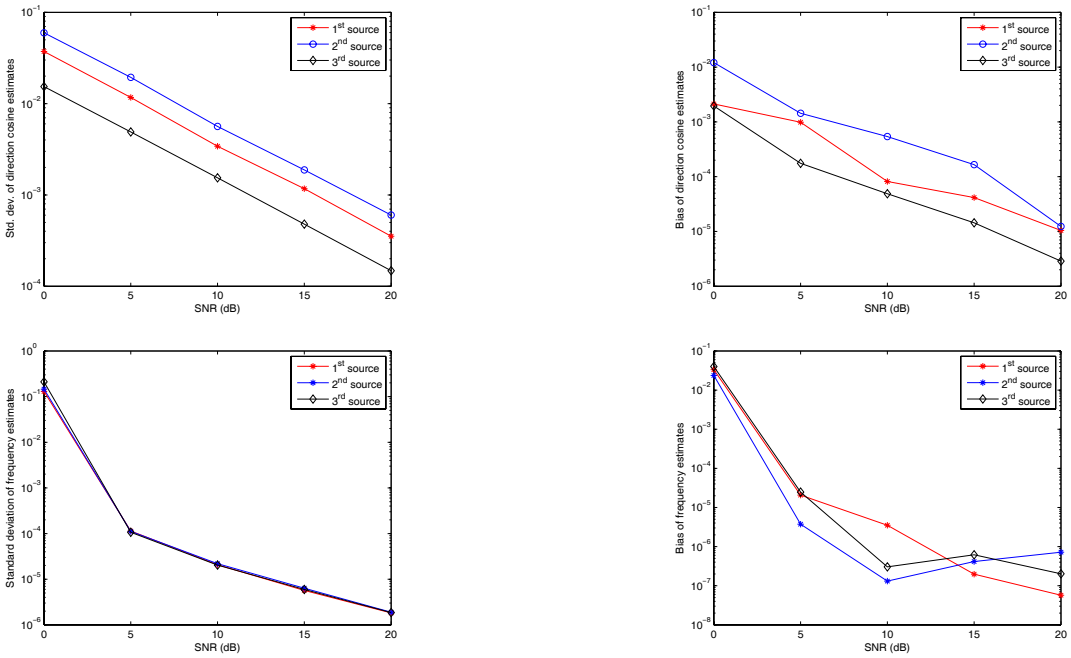

Figure 3: Standard deviation and bias of direction cosine and frequency estimates for $K = 3$, $M = 4$ with temporal sampling rate of $F_{Nyq}/4$ (from left to right, top to bottom): standard deviation of direction estimates, bias of direction cosine estimates, standard deviation of frequency estimates, and bias of frequency estimates.

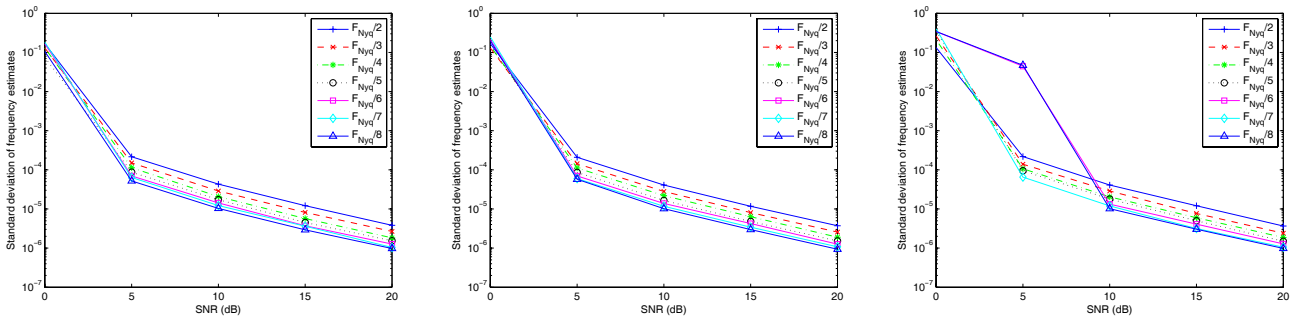

Figure 4: Standard deviation of frequency estimates for $K = 3$, $M = 4$ for different temporal sampling (left to right): first source, second source, and third source.

and frequency estimates for the 3 sources. As the figures show, the direction cosine and frequency estimates can still be accurately (and unambiguously) estimated even when the temporal sampling is less than half of the Nyquist rate. Figure 4 shows the standard deviation of all three frequency estimates when different sub-Nyquist rates were used. The parameters used are identical to the ones in Figure 3. The figures show that all the frequencies can be unambiguously estimated and the accuracy of the estimates increases as the SNR goes up.

4. CONCLUSION

Two novel algorithms have been proposed to solve the frequency ambiguity problems in ESPRIT based joint 2-D DOA and frequency estimation when the interelement spacing is more than $\lambda_{min}/2$ and when the temporal sampling rate is below half of the Nyquist rate. Our analysis and simulation results showed that when the interelement spacing is more than $\lambda_{min}/2$, it is possible to obtain 2-D DOA and frequency estimates by restricting the temporal sampling to no less than half of the Nyquist rate. This assumes that the receiver has knowledge about the upper bound of the incoming signal's frequency. This has applications in distributed sensor array where the sensors can be located sparsely over a wide region of space. In addition, if $\Delta x \leq \lambda_{min}/2$, we have shown that it is still possible to obtain unambiguous estimates when sub-Nyquist rates are used.

REFERENCES

[1] A.J. van der Veen, M.C. Vanderveen and A. Paulraj, "Joint Angle and Delay Estimation Using Shift-Invariance Techniques", *IEEE Trans. Signal Processing*, vol.46(2), pp. 405-418, Feb. 1998.

[2] M.D. Zoltowski and C.P. Matthews, "Real-Time Frequency and 2-D Angle Estimation with Sub-Nyquist Spatio-Temporal Sampling", *IEEE Trans. on Signal Processing*, vol. 42(10), pp. 2781-2794, Oct. 1994.

[3] A.N. Lemma, A.J. van der Veen and E.F. Deprettere, "Multiresolution ESPRIT Algorithm", *IEEE Trans. on Signal Processing*, vol. 47(6), pp. 1722-1726, Jun. 1999.

[4] J. Li, "Direction and Polarization Estimation Using Arrays with Small Loops and Short Dipoles", *IEEE Trans. on Antennas and Propagation*, vol. 41(3), pp. 379-387, Mar. 1993.

[5] A. Nehorai and E. Paldi, "Vector-Sensor Array Processing for Electromagnetic Source Localization", *IEEE Trans. on Signal Processing*, vol. 42(2), pp. 376-398, Feb. 1994.

[6] K.T. Wong and M.D. Zoltowski, "Uni-Vector-Sensor ESPRIT for Multisource Azimuth, Elevation, and Polarization Estimation", *IEEE Trans. on Antennas and Propagation*, vol. 45(10), pp. 1467-1474, Oct. 1997.

[7] M.D. Zoltowski and K.T. Wong, "ESPRIT-Based 2-D Direction Finding with a Sparse Uniform Array of Electromagnetic Vector Sensors", *IEEE Trans. on Signal Processing*, vol. 48(8), pp. 2195-2204, Aug. 2000.

[8] R. Roy and T. Kailath, "ESPRIT-Estimation of Signal Parameters Via Rotational Invariance Techniques", *IEEE Trans. on Acoustics, Speech, and Signal Processing*, vol. 37(7), pp. 984-995, Jul. 1989.

[9] K.-C. Tan, K.-C. Ho and A. Nehorai, "Uniqueness Study of Measurements Obtainable with Arrays of Electromagnetic Vector Sensors", *IEEE Trans. on Signal Processing*, vol. 44(4), pp. 1036-1039, Apr. 1996